Chew, K. F., Derbyshine, W., Logan, N., Norbury, A. H., & Sinha, A. I. P. (1970) *J. Chem. Soc. D*, 1708.
Coleman, J. E. (1967a) *Nature (London) 214*, 193-194.
Coleman, J. E. (1967b) *J. Biol. Chem. 242*, 5212-5219.
Evelhoch, J. L., Bocian, D. F., & Sudmeier, J. L. (1981) *Biochemistry 20*, 4951-4954.
Forster, D., & Goodgame, D. M. L. (1963) *J. Chem. Soc.*, 2790-2798.
Forster, D., & Goodgame, D. M. L. (1964) *J. Chem. Soc.*, 262-267.
Ghosh, N. N., & Majumder, M. N. (1963) *J. Indian Chem. Soc. 40*, 945-952.
Grunwald, E., & Fong, D. W. (1972) *J. Am. Chem. Soc. 94*, 7371-7377.
Kakeya, N., Aoki, M., Kamada, A., & Yata, N. (1969) *Chem. Pharm. Bull. 17*, 1010-1018.
Kannan, K. K., Vaara, I., Notstrand, B., Lovgren, S., Borell, A., Fridborg, K., & Petef, M. (1977) in *Drug Action at the Molecular Level* (Roberts, G. C. K., Ed.) pp 73-91, University Park Press, Baltimore, MD.
Khalifah, R. G. (1971) *J. Biol. Chem. 246*, 2561-2573.
Kidani, Y., Noji, M., & Koike, H. (1973) *Yakugaku Zasshi 93*, 1391-1393.
King, R. W., & Burgen, A. S. V. (1970) *Biochim. Biophys. Acta 207*, 278-285.
Kumar, K., King, R. W., & Carey, P. R. (1976) *Biochemistry 15*, 2195-2202.
Lindskog, S., & Nyman, P. O. (1964) *Biochim. Biophys. Acta 85*, 462-474.
Lindskog, S., & Thorslund, A. (1968) *Eur. J. Biochem. 3*, 453-460.
Maren, T. H., & Couto, E. O. (1979) *Arch. Biochem. Biophys. 196*, 501-510.
Nee, M. W., & Roberts, J. D. (1982) *Biochemistry 21*, 4920-4926.
Nostrand, B., Vaara, I., & Kannan, K. K. (1975) in *Isoenzymes I, Molecular Structure* (Markert, C. L., Ed.) p 575, Academic Press, New York.
Osborne, W. R. A., & Tashian, R. E. (1975) *Anal. Biochem. 64*, 297-303.
Pesando, J. M. (1975) *Biochemistry 14*, 675-688.
Pocker, Y., & Sarkanen, S. (1978) *Adv. Enzymol. Relat. Areas Mol. Biol. 47*, 149-274.
Pocker, Y., & Diets, T. L. (1982) *J. Am. Chem. Soc. 104*, 2424-2434.
Price, G. H. (1979) *Clin. Chim. Acta 94*, 211-217.
Price, G. H. (1980) *Clin. Chim. Acta 101*, 313-319.
Rickli, E. E., & Edsall, J. T. (1962) *J. Biol. Chem. 237*, PC 258.
Schuster, I. I., Doss, S. H., & Roberts, J. D. (1978) *J. Org. Chem. 43*, 4693-4696.
Stark, G. R. (1972) *Methods Enzymol. 25*, 579.
Taylor, P. W., King, R. W., & Burgen, A. S. V. (1970) *Biochemistry 9*, 3894-3902.

pH-Dependent Polymerization of a Human Leukocyte Interferon Produced by Recombinant Deoxyribonucleic Acid Technology†

Steven J. Shire

ABSTRACT: The pH-dependent polymerization of human leukocyte interferon A produced by recombinant DNA technology was investigated by potentiometric hydrogen ion titration and sedimentation velocity analytical ultracentrifugation. The titration curve is completely reversible from pH 6.2 to 2.5. Analysis of the side-chain carboxyl residues by using the Linderstrøm-Lang equation yields a linear plot from pH 5.2 to 3.5. The resulting pK_{int} and W values are 4.66 ± 0.06 and 0.036 ± 0.004, respectively. The titration curve from pH ~9.6 to 7 is also reversible. However, the reverse titration from pH 7 to 6 results in a time-dependent variation of pH. Sedimentation velocity analysis yields an increase in the corrected sedimentation coefficient, $s_{20,w}$, from 2.0 to 4.0 S over a pH range of 2.5-9 at 0.38-0.25 mg/mL total protein concentration. The concentration dependence of the sedimentation coefficient at pH 7.0 over the range of 0.05-6.0 mg/mL results in a positive slope which is typical for self-aggregating systems. This aggregation phenomenon is discussed in terms of its ramifications for interferon therapy.

Interferons are an important class of proteins which exhibit antiproliferative and antiviral activity (Stewart, 1979). These proteins isolated from cell cultures are of insufficient purity and quantity to be studied by biophysical techniques. With the advent of recombinant DNA technology, we are now able to produce large amounts of protein of high purity. This paper deals with a study of the amino acid ionizations and possible linkage to self-polymerization of a human leukocyte interferon, designated LeIF-A,[1] produced by recombinant technology.

LeIF-A is one of eight related human leukocyte interferons (Mantei et al., 1980; Streuli et al., 1980; Goeddel et al., 1980, 1981) and has been characterized biochemically by determining amino acid composition, molecular weight (by NaDodSO$_4$-polyacrylamide gel electrophoresis), N-terminal sequence (first 35 residues)(Wetzel et al., 1981), and disulfide linkages (Wetzel, 1981). Recent circular dichroism and ultraviolet absorption measurements of LeIF-A have probed the well-known acid stability of the molecule in terms of changes in secondary and tertiary structures (Bewley et al., 1982).

The self-polymerization of proteins is a common occurrence which very often plays a role in the biological function of the

† From the Department of Vaccine Development, Genentech, Inc., South San Francisco, California 94080. *Received September 7, 1982.* Genentech Contribution No. 126.

[1] Abbreviations: LeIF-A, human leukocyte interferon A produced by recombinant DNA technology; K(H)PO$_4$, potassium orthophosphate, mono- and dibasic salts; NaDodSO$_4$, sodium dodecyl sulfate; Tris, tris(hydroxymethyl)aminomethane; I, ionic strength.

0006-2960/83/0422-2664$01.50/0

molecule (Oosawa & Asakura, 1975). Proteins consist of several ionizable groups, and the electrostatic interactions between these groups may be involved in controlling the assembly behavior. In particular, the ionization state of the constituent amino acids can determine when and how these forces affect assembly. The state of ionization is dependent on the ionic environment such as pH and ionic strength. Different assembly systems such as tropomyosin (Bailey, 1948; Asai, 1961), tobacco rattle virus coat protein (Fritsch et al., 1973), and tobacco mosaic virus coat protein (Caspar, 1963) exhibit different polymerization behavior as a function of ionic strength. This suggests that electrostatic interactions can be involved in either a stabilization or a destabilization of the polymer state depending on the distribution and quantity of the interacting charges. The conformation and ionization behavior of titratable residues of a protein can be probed over a wide pH range by hydrogen ion titration (Tanford, 1962; Van Os et al., 1972). Additional information regarding the protein's molecular size in solution can be obtained from analytical ultracentrifugation. Here we present the first characterization of assembly properties and ionization behavior of LeIF-A as determined by potentiometric hydrogen ion titrations and sedimentation velocity analytical ultracentrifugation.

Materials and Methods

Materials. The preparation and purification of LeIF-A were as described previously (Wetzel et al., 1981) with additional purification on a monoclonal antibody column (Staehelin et al., 1981). The homogeneity of the sample was ascertained by $NaDodSO_4$–polyacrylamide gel electrophoresis and isoelectric focusing. LeIF-A samples were dialyzed against 0.1 N KCl, concentrated by ultrafiltration (YM10 membrane, Amicon, Inc.), and, after freezing in liquid N_2, stored frozen until ready for use. The protein samples were thawed prior to an experiment and centrifuged in order to remove small amounts of denatured protein (<1%).

Protein concentrations were determined in 0.1 M Tris-HCl at pH 8.2 by using an $E_{280nm}^{0.1\%,1cm}$ of 1.06 (Bewley et al., 1982), and interferon activity was determined by a cytopathic effect assay as previously described (Wetzel et al., 1981).

All chemicals were reagent grade, and glass bidistilled water was used in all experiments. Stock 0.1 N KOH (Baker Chemicals, Analyt.-Dilut It) was standardized against primary standard potassium hydrogen phthalate (National Bureau of Standards), and 0.1 N HCl (Baker Chemicals) was standardized to phenolphthalein end point with the standardized base.

Potentiometric Hydrogen Ion Titrations. The titration apparatus similar to a previous experimental design (Shire et al., 1974a) consisted of a water-jacketed glass titration vessel (~1.5-mL capacity) with a glass electrode (Radiometer G2222B, semimicro) and a water-jacketed calomel reference electrode (Radiometer K4018) connected by a KCl salt bridge. The KCl salt bridge was prepared by filling a thin Teflon tube with a solution of saturated KCl in 1% agar. An air-driven magnetic stirrer was placed under the vessel, and the titration assembly with stirrer was enclosed within a Faraday box, grounded, and connected to a Radiometer pHM84 meter. A calibrated microburet (Agla brand, Wellcome Research Laboratories) fitted with a glass syringe and a thin polyethylene tube was used to deliver acid or base as required. Interferon samples at 1–1.5 mg/mL were dialyzed exhaustively against 0.1 N KCl. Nitrogen gas was bubbled through the dialyzate in order to remove CO_2 during the final 24 h of dialysis prior to removing the LeIF-A for titration. The pH scale was linearized with primary standard phosphate and phthalate buffers (National Bureau of Standards) prior to introduction of 0.75 mL of interferon solution into the titration vessel. Nitrogen gas was scrubbed in glass bidistilled water, passed over a resin to remove contaminating CO_2 (Mallcasorb, Mallinckrodt Inc.), and bubbled through 0.1 N KCl at 25 ± 0.1 °C before it was allowed to flow continuously over the sample surface at 25 °C. The 0.1 N KCl dialyzate was titrated separately under the same titration conditions.

Sedimentation Velocity Experiments. Analytical model E ultracentrifuges (Spinco, Beckman Inc.) equipped with schlieren and photoelectric scanner optics were used for sedimentation analysis at 23 °C. Samples were centrifuged at either 52 000 or 60 000 rpm in an AnD rotor. Concentrated interferon samples (1–6.0 mg/mL) were either dialyzed or diluted into the appropriate buffers. Buffers ranging in pH from 2.5 to 10.0 were prepared as 0.01 M ionic strength in buffer salts (Gly–HCl, pH 2.5 and 3.3, acetic acid–KOH, pH 5.0, $K(H)PO_4$,[1] pH 5.9, 6.9, and 7.0, Tris-HCl, pH 8.8, and Gly–KOH, pH 10.0) and 0.09 M ionic strength KCl. Sedimentation coefficients were determined by standard analysis by using the midpoints of the boundaries measured with the photoelectric scanner, and coefficients were corrected in the usual manner (Schachman, 1959). The assumption that the major contribution to the correction is from the 0.09 M KCl resulted in a correction factor of 0.949.

Computations of Titration Curves. All computations were performed on a Vax 11/780 (Digital Corp.) digital computer by inputting intrinsic pK values, pK'_{int}, for amino acid residues in a hypothetically discharged protein. This set of pK values has been used previously in a discrete charge-modified Kirkwood–Tanford computation, and the rationale for the selection of these values has already been discussed in detail (Shire et al., 1974a,b; Matthew et al., 1978). The average charge, $\bar{Z}$, at any pH, is computed by subtracting the contribution of all titratable groups from the maximum protein charge, Z_{max} (Tanford, 1962), so that

$$\bar{Z} = Z_{max} - \sum_i N_i \alpha_i \quad (1)$$

where N_i is the number of amino acid residues of the ith kind with a fractional dissociation of α_i. Computation of α_i follows from the usual mass balance expression:

$$pH - \log [\alpha_i/(1 - \alpha_i)] = (pK_i)'_{int} \quad (2)$$

The equations can also be manipulated to yield an expression for the differential titration curve (DeBruin & Van Os, 1968) so that

$$\frac{dpH}{d\bar{Z}} = \frac{1}{2.303 \sum_i N_i \alpha_i (1 - \alpha_i)} \quad (3)$$

Equation 3 was used to compute theoretical differential titration curves for comparison with the experimentally derived curves.

Computations of s vs. C Curves. Simulations of the weight-average sedimentation coefficient as a function of concentration were performed by using an algorithm to compute monomer concentration as described by Cox (1978). The coefficient which determines the hydrodynamic concentration dependence of the sedimentation coefficient was set equal to 0.01 L/g. Association constants, $K(I)$, relating aggregation of n monomers at a concentration of C_1 to an n-mer at a concentration of C_n are expressed on a weight scale so that $K(n) = C_n/C_1^n$ and were inputted into the algorithm. The intrinsic sedimentation coefficient for monomer was computed as described under Results and Discussion, and sedimentation

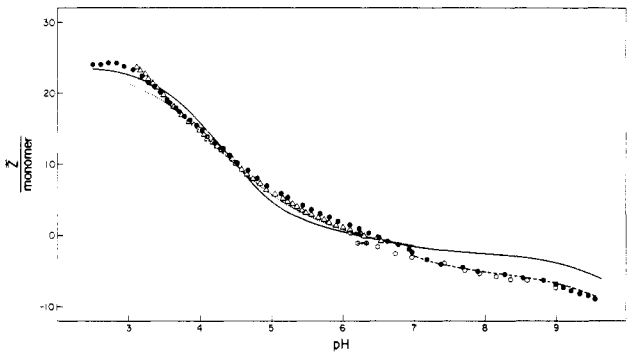

FIGURE 1: Hydrogen ion potentiometric titration of human leukocyte interferon A at 25 °C and 0.1 M KCl. The pH time dependence is indicated by arrows and encircled crosses. $\bar{Z}$ is the average charge on the protein monomer of molecular weight 19 400. (●) Titration from pH 2.5 to 10, protein concentration at 1.0 mg/mL; (○) reverse titration from pH 11 to ~6.2; (△) reverse titration from pH 2.5 to ~6.2 after forward titration from pH 6.2 to 2.5, protein concentration at 1.2 mg/mL. Solid, dashed, and dotted lines are titration curves computed by using the parameters in Table I.

coefficients of the aggregates were computed as $s_{n\text{-mer}} = s_{\text{monomer}} n^{2/3}$ which is tantamount to assuming equal frictional ratios for all the aggregates.

Results and Discussion

Hydrogen Ion Titration Curve. The titration curve for LeIF-A at 25 °C and 0.1 M KCl (expressed as the average charge per monomeric protein unit of 19 400 daltons, vs. pH) is shown in Figure 1. The equivalents of titrant bound per monomer unit are equated to the average net charge of the protein by assuming that there is no great degree of counterion binding to specific protein sites. Generally, the pH of the dialyzed protein was between 6.0 and 6.2, but occasionally pH values between 5.7 and 6.0 were obtained. When this occurred, the protein was rapidly titrated to pH 6.1, and the shape of the subsequently derived titration curve was found to be identical with those with a starting pH above 6.0. Previous isoelectric focusing experiments (Wetzel et al., 1981) found the p*I* of LeIF-A to be 6.1, and thus, pH values of 6.1–6.2 were assumed to be isoelectric. Titration experiments from the p*I* down to pH 2.5 yielded results identical with the reverse curve (open triangles) shown in Figure 1 and were omitted for clarity. The fact that the titration is reversible is significant since leukocyte interferon bioactivity is known to be acid stable (Stewart, 1979). Since the bioassay is performed over a period of 24 h at pH 7.0, any information regarding the rate of reversibility of any structural changes at low pH is lost. Circular dichroism and UV absorption measurements at pH 2.5 and 7.0 (Bewley et al., 1982) indicate that there are conformational changes which to a large degree are reversible. The reversibility of the titration in the acidic region demonstrates that these conformational changes are rapid in the time scale of the titrations (order of minutes per titrant addition).

The open circles in Figure 1 show the reverse titration of LeIF-A from pH ~10 to the p*I*. This titration in the basic region is reversible until pH 7.0. From pH 7.0 to 6.0, there is a noticeable time-dependent variation of pH of the order of minutes. This dependence on time manifests itself as a hysteresis loop as seen in Figure 1. The pH was unstable during these measurements as reflected by the arrows and encircled crosses. The other data points in the loop were also time dependent but were not allowed to drift to a stable pH value before the next addition of titrant.

The solid curve in Figure 1 is a computed titration curve determined by using the parameters given in Table I. This

Table I: Parameters Used To Compute Titration Curves in Figure 1 Using Equations 1 and 2[a]

	solid line		dotted line		dashed line	
amino acid	pK_i[b]	N_i	pK_i[b,c]	N_i	pK_i[b]	N_i
Asp	4.0	8	4.66	22	4.0	8
Glu	4.5	14			4.5	14
C terminal	3.6	1	3.6	1	3.6	1
His	6.3	3	6.3	3	6.3	3
N terminal	8.0	1	8.0	1	8.0	1
Tyr	10.0	5	10.0	5	10.0	5
Lys	10.4	11	10.4	11	10.4	8
					7.0	3
Arg	12.0	9	12.0	9	12.0	9
Z_{max}	24		24		24	
W	0.0		0.037		0.0	

[a] Parameters are defined in the text. [b] Based on pK_{int} values used by Matthew et al. (1978). [c] Based on side-chain carboxyl pK_{int} determined from Figure 4.

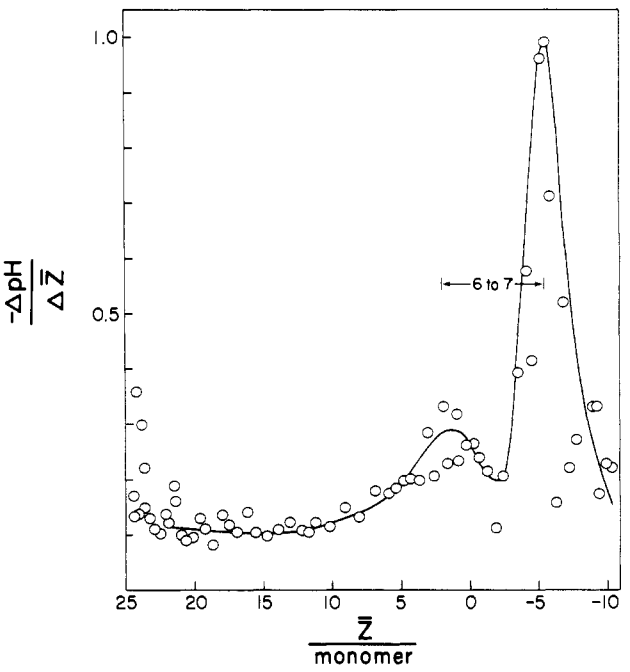

FIGURE 2: Differential titration curve for human leukocyte interferon A obtained from titration data at 25 °C and 0.1 M KCl in Figure 1 (○). The smooth curve is hand drawn through the data points.

computed curve assumes independent titrations without interactions between titratable residues. The discrepancy between the computed curve and experimental data in the basic region of the titration is substantial and indicates that major shifts in "normal" p*K* values of basic groups have occurred. This is demonstrated by the dashed line in Figure 1 which is a computed curve determined by using the same set of p*K* values as for the solid curve except that three lysine residues have p*K* values shifted from 10.4 to 7.0 (see Table I). Essentially identical results are obtained by shifting the p*K* values of three of the five tyrosine residues from 10.0 to 7.0 (data not shown).

In Figure 2, the titration data are plotted as a derivative curve, $-\Delta pH/(\Delta \bar{Z})$ vs. $\bar{Z}$, as suggested by previous investigators (Van Os et al., 1972; DeBruin & Van Os, 1968). The distance on the $\bar{Z}$ axis from Z_{max}, the maximum net charge of 24, to the first maximum peak position is equivalent to the number of residues titrating in the acidic region of the curve. The data indicate that at least 22 and possibly all 23 carboxyl residues are titrating in the acidic region of the curve. The amount of scatter in the data precludes making a definitive statement

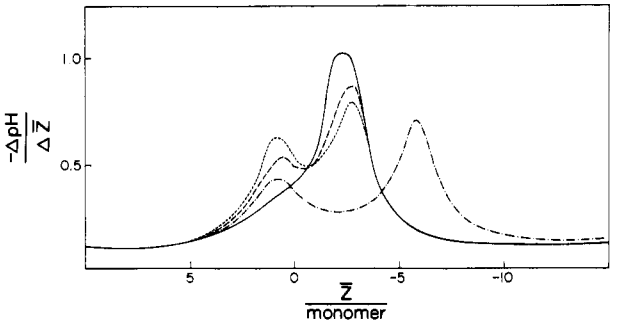

FIGURE 3: Differential titration curves (see text for details) computed by using the following parameters: (—) same parameters given in Table I for solid line; (- - -) same parameters except three His at pK = 6.8; (···) same parameters except three His at pK = 7.0; (-·-) same parameters except three His at pK = 7.0 and three Lys at pK = 7.0.

regarding the possibility of the presence of at most one abnormally titrating carboxyl residue.

The distance on the $\bar{Z}$ axis between both maximum peak positions is an indication of the number of amino acid residues titrating in the neutral region of the curve. Figure 2 shows that there are six to seven residues titrating in this region, two to three greater than can be accounted for by the amino acid composition.

Computations of the differential titration curve by using eq 3 and the same set of parameters used to compute the solid curve in Figure 1 resulted in the solid curve shown in Figure 3 where the first peak is essentially a shoulder and the second peak occurs at a $\bar{Z}$ value of −2 to −3. The computations were repeated with the same data set used to compute the solid curve except that the histidine pK values were set at 6.8 or 7.0 (dashed and dotted curves, respectively, in Figure 3). As can be seen in Figure 3, as the histidine pK values are increased, the shoulder on the ascending limb of the curve becomes accentuated, resulting in a distinct peak. A comparison of these computed curves with the experimentally derived curve (Figure 2) shows that the histidine residues titrate with pK values greater than 6.3, more likely in the range of 6.8–7.0. Another computation with the same pK data set but with three histidine and three lysine residues with pK values of 7.0 yielded the dashed dotted curve shown in Figure 3. This curve is similar in shape and axis spacing to the experimentally derived curve (Figure 2). The relative heights of the two computed peaks are not the same as those determined experimentally. However, an increase in the relative height would result if the three histidine residues were assigned slightly lower pK values than 7.0 as shown by the three curves computed with different histidine pK values (Figure 3).

Analysis of Side-Chain Carboxyl Titrations. Since very few residues other than carboxyl residues titrate in the acidic region of protein titration curves, it is possible to analyze the side-chain carboxyl titrations by using the Linderstrøm-Lang equation (Linderstrøm-Lang, 1924) (eq 4) in a semiempirical manner:

$$\mathrm{pH} - \log [\alpha_i/(1 - \alpha_i)] = (\mathrm{p}K_i)_{\mathrm{int}} - 0.868W\bar{Z} \qquad (4)$$

where W, the electrostatic interaction parameter, is related to the electrostatic free energy, W_{el}, of the macromolecule so that $W = W_{\mathrm{el}}/(kT)$; k is the Boltzmann factor, and T is the temperature (Tanford, 1961). The parameter W is dependent on structural parameters of the particular geometrical model chosen to represent the protein. If the protein is assumed to be a sphere of radius R_0 with an average net charge $\bar{Z}$ smeared evenly over the surface, then

$$W_{\mathrm{sphere}} = [\epsilon^2/(2DkTR_0)][1 - \kappa R_0/(1 + \kappa a)] \qquad (5)$$

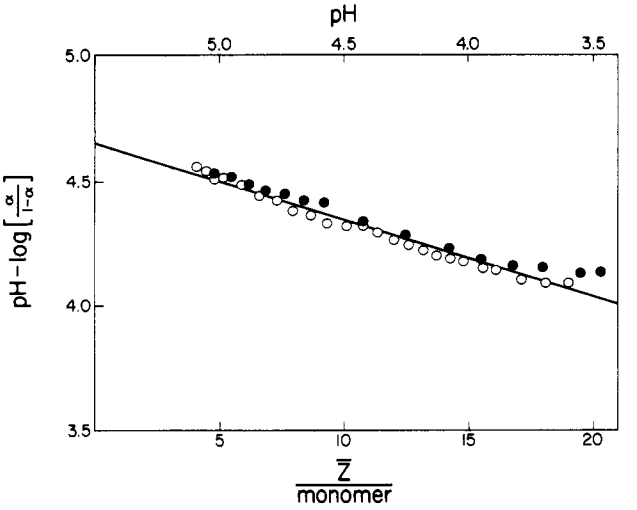

FIGURE 4: Titration data for side-chain carboxyl groups at 25 °C and 0.1 M KCl. Average values determined from six separate experiments are $\mathrm{p}K_{\mathrm{int}} = 4.66 \pm 0.06$ and electrostatic interaction parameter $W = 0.036 \pm 0.004$. The pH at $\bar{Z}$ as determined from the potentiometric curve (Figure 1) is given on the top axis. (○) and (●) are data points from two separate experiments.

where ϵ = the electronic charge, D = the dielectric constant of water at temperature T, a = the distance of closest approach (R_0 + 2 Å), and κ = the Debye screening parameter. The radius R_0 can be estimated with (Tanford, 1962)

$$R_0 = [[3/(4\pi)](M_{\mathrm{p}}/N_0)(\bar{V}_{\mathrm{p}} + \delta_{\mathrm{w}}V_{\mathrm{w}}^0)]^{1/3} \qquad (6)$$

where M_{p} = the protein molecular weight, N_0 = Avogadro's number, $\bar{V}_{\mathrm{p}}$ = the partial specific volume of the proteins, δ_{w} = grams of water bound per gram of protein, and V_{w}^0 = the partial specific volume of water.

The titration curve yields values of $\bar{Z}$ at a particular pH value. Values of α_i are computed from $\bar{Z}$ by estimating the number of side-chain carboxyl groups which titrate in the acidic region of the titration curve. Subtraction of the C-terminal carboxyl titration from the experimental titration data results in a titration curve of only the side-chain carboxyl residues provided there are no abnormally ionizing noncarboxyl side chains. Following Tanford (1962), a reasonable value for the carboxyl-terminal pK of 3.6 is chosen, and it is assumed that all 22 side-chain carboxyls ionize identically as one class of titratable residues. The left side of eq 4 is then plotted vs. the average net charge, and the resulting intercept and slope yield the intrinsic pK value and the electrostatic interaction parameter, W, respectively. The results of this analysis are shown in Figure 4 for two separate titrations. It is apparent that over the pH range of ~3.5–5.2 the parameter W is a constant and results in a linear plot. This demonstrates that from pH 5.2 to 3.5 the molecule does not undergo any large overall structural change. Changes in conformation which result in large changes of molecular geometry will in turn result in changes in the parameter W (eq 5). Below pH 3.5, the plot deviates from linearity, demonstrating that the molecule undergoes a structural change. This observation is consistent with the large changes in secondary structure determined by circular dichroism measurements at pH 2.5 (Bewley et al., 1982). Linear regression analysis of the linear region of the plot for six different titrations yields $\mathrm{p}K_{\mathrm{int}} = 4.66 \pm 0.06$ and $W = 0.036 \pm 0.004$. This $\mathrm{p}K_{\mathrm{int}}$ value is in good agreement with $\mathrm{p}K_{\mathrm{int}}$ values obtained for side-chain carboxyl residues of other proteins (Tanford, 1962). The $\mathrm{p}K_{\mathrm{int}}$ value resulting from this analysis should not be confused with the choice of $\mathrm{p}K'_{\mathrm{int}}$ values used in the computations of Figures 1 and 2 since the

former is an intrinsic value defined when $\bar{Z}$, the average net charge of the protein, is zero rather than for a hypothetically discharged state (Shire et al., 1974b).

The experimentally determined value of W can be compared to a value of W_{sphere} computed from eq 5 by using a radius, R_0, estimated from eq 6. Values of $\bar{V}_p = 0.73$, $\delta_w = 0.2$, $V_w^0 = 1.0$ (Tanford, 1962) result in an estimated R_0 of 19.3 Å. At 0.1 M ionic strength, W_{sphere} is 0.07, which is 49% greater than the experimentally determined value of 0.036. Tanford (1962) has discussed the reasons for differences between calculated and experimentally determined values of W. He concludes that the differences between experiment and theory are not significant for experimental values of W up to 33% lower than those predicted by eq 5. The difference between experiment and theory obtained for LeIF-A is somewhat greater than 33%. The computation for W was based on a spherical geometry, and since LeIF-A is not necessarily spherical, it is instructive to recompute W for an equivalent volume cylinder from eq 7 (Hill, 1955) where L = cylinder

$$W_{cylinder} = [\epsilon^2/(DLkT)]\left[\frac{K_0(\kappa a)}{\kappa a K_1(\kappa a)} + \ln\frac{a}{R}\right] \quad (7)$$

length, R = cylinder radius, and K_0 and K_1 are zero- and first-order Bessel functions. Axial ratios of 4:1 and 8:1 result in computed values of $W = 0.084$ and 0.062, respectively. It is unlikely that LeIF-A is an extremely elongated molecule with axial ratios greater than 8:1, and thus, cylindrical geometry cannot account for the difference between experiment and theory.

An alternative explanation for the lower experimental value of W is that the molecule is less compactly folded than expected on the basis of eq 6. A radius R_0 of ~28 Å would result in a value of W of 0.036. The protein would thus be expanded to about 3 times the volume based on the estimated hydrodynamic radius of 19.3 Å from eq 6. Although this large expansion appears unlikely, it may well indicate that throughout the acidic titration range LeIF-A exists in a more expanded geometry than expected on the basis of its molecular weight. Since the Linderstrøm-Lang plots are linear, the change in hydrodynamic radius cannot occur during the titration of the carboxyl residues. The actual values for W and hence the hydrodynamic radius are dependent on the assumed number of carboxyl residues which titrate with identical ionization constants (Marini & Martin, 1980). Variation of the number of side-chain carboxyl residues as well as the assumed pK values results in lower values of W (S. J. Shire, unpublished calculations) and therefore cannot account for the difference between theory and experiment.

The titration curve computed by using eq 4 in an iterative fashion (Tanford & Roxby, 1972) with $W = 0.036$ and $pK_{int} = 4.66$ results in a very good fit of the data from pH 3.5 up to pH 6.6 as shown by the dotted curve in Figure 1. Beyond pH 7.0, this curve is essentially identical with the solid curve. The range of pH over which this computed curve is in agreement with data is significant because the W parameter was obtained only for the side-chain carboxyl residues and not for the histidine residues. In the pH region of 6.2–7.0 where the histidine residues are titrating (see Figure 1), the protein has a slight negative charge. Equation 4 for a smeared-charge model predicts that electrostatic interactions would result in an increased pK value, the exact magnitude of which is determined by the values of W and $\bar{Z}$. The computed curve (dotted curve in Figure 1) is in good agreement with the experimental data up to pH 6.6, and thus, the side-chain carboxyl W value adequately accounts for the data. Since this analysis is based on a smeared-charge distribution model, this suggests that the histidine residues are exposed to a symmetrical charge environment whose local environment is not altered drastically over the pH range of 6–7. The fit of the data by the computed curve is also consistent with the notion that the effective pK values of the histidine residues are somewhat higher than the intrinsic pK value of 6.3 used in the original calculation.

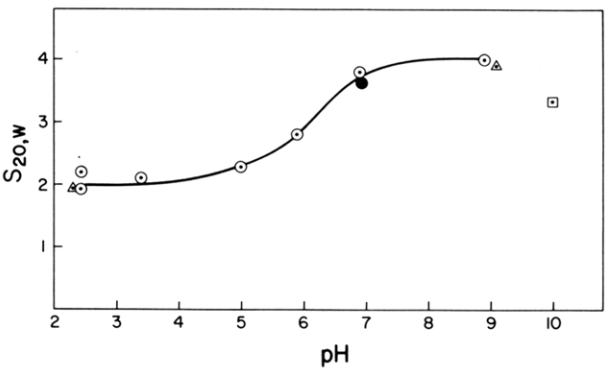

FIGURE 5: Corrected sedimentation coefficients, $s_{20,w}$, for human LeIF-A at ~23 °C and I = 0.1 M KCl as a function of pH. All solutions are buffered with I = 0.01 M buffer salts, and the remaining ionic strength is made up with KCl. Protein concentrations are as follows: (○) 0.38 mg/mL; (●) 0.26 mg/mL; (△) 0.25 mg/mL; (□) 0.32 mg/mL.

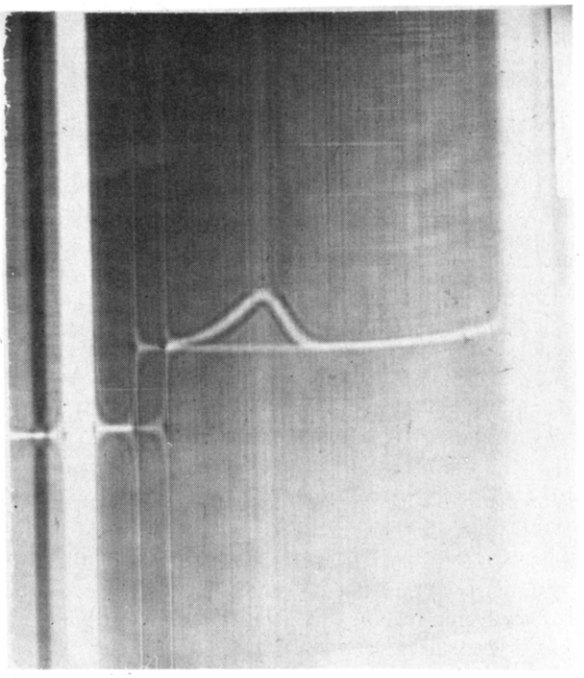

FIGURE 6: Schlieren photograph of LeIF-A at 3.2 mg/mL, 23 °C, pH 7.0 [I = 0.01 M $K(H)PO_4$ + 0.09 M KCl], ~30 min after coming to speed at 60 000 rpm in an AnD rotor. Sedimentation is from left to right.

Sedimentation Velocity Experiments. LeIF-A diluted into various pH buffers (see Materials and Methods) was analyzed by sedimentation velocity at 22.6 °C at a concentration range of 0.25–0.38 mg/mL. The pH dependency of the corrected sedimentation coefficient, $s_{20,w}$, is shown in Figure 5. Over a pH range of 2.0–9.0, the sedimentation coefficient increases from a value of 2.0 S to 4.0 S with an apparent pK of 6.0. As can be seen in Figure 6, the schlieren boundary is a highly skewed asymmetric boundary and undoubtedly represents a reaction boundary (Gilbert, 1959) rather than a unique structural aggregate. Thus, the sedimentation coefficients are weight-average values for a rapidly equilibrating system. It

Table II: Computations of Sedimentation Coefficients Using Equations 8 and 9 and R_0 = 19.3 Å[a]

(A) Monomer

a:b	$s_{20,w}$ (S)
1:1	2.4
2:1	2.3
3:1	2.2
4:1	2.0
5:1	1.9
6:1	1.8

(B) Aggregate

$s_{20,w}$ (S)	n-mer	model	b	a
3.7	dimer, linear		19.3	38.6
4.5	trimer, linear	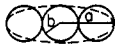	19.3	57.9
5.2	trimer, cyclic (planar)		19.3	43.4
5.2	tetramer, linear	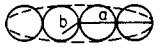	19.3	77.2
6.7	tetramer, planar		19.3	46.6
4.8	tetramer, tetrahedral		38.6	38.6

[a] The model parameters a and b refer to the semimajor and semiminor axes, respectively, for a spheroid which approximates the structural model depicted.

is still possible to estimate the sedimentation coefficient for a discrete aggregate which contributes to the equilibrium.

Estimates of the sedimentation coefficients for molecules can be made by using the traditional approach of combining equations for the frictional coefficient of a prolate ellipsoid (Perrin, 1936) with the sedimentation velocity equation in terms of molecular weight and frictional coefficient (Caspar, 1963; Schachman 1959), yielding

$$s = \frac{(1 - \bar{V}_p\rho)M_p}{6\pi N_0 \eta R_0} \frac{(b/a)^{2/3} \ln \{[1 + (1 - b^2/a^2)^{1/2}]/(b/a)\}}{(1 - b^2/a^2)^{1/2}} \quad (8)$$

where η and ρ are the viscosity and density of the solution, respectively, and $R_0 = (ab^2)^{1/3}$ where a and b are the semimajor and semiminor axes, respectively, of the prolate ellipsoid.

For a spherical geometry where $b = a$, eq 8 reduces to

$$s = \frac{(1 - \bar{V}_p\rho)M_p}{6\pi N_0 \eta R_0} \quad (9)$$

If infinite dilution in water (ρ and η of water at 20 °C) is assumed, the resulting computed values of $s_{20,w}$ are values which are presented in Table II for prolate ellipsoids of varying ratios $a:b$, R_0 = 19.3 Å, and $\bar{V}_p$ = 0.73. The computed value for monomer varies from 1.8 to 2.4 S, depending on the axial ratio, and is in good agreement with the experimental $s_{20,w}$ value of 2.0 S at 0.25 mg/mL protein concentration obtained at a pH of 2.5.

Computations of sedimentation coefficients for various size aggregates can be simplified by assuming spherical geometry for the interferon monomeric unit. If it is assumed that $\bar{V}_p$ is unchanged upon aggregation, the computed sedimentation coefficient, $s_{n\text{-mer}}$, for an n-mer is equivalent to $nM_p s_{spheroid}$ where $s_{spheroid}$ is the computed sedimentation coefficient for a spheroid used to approximate the overall geometry of the aggregate. Although more exact computations than these are possible by using the Kirkwood theory (1949, 1954) or extensions of the theory (Bloomfield et al., 1967), the uncertainty in the value for the radius of the approximating sphere for the monomer, as well as the assumption of spherical geometry for the monomer, does not warrant more involved calculations than those presented here. Table II presents values for various aggregates up to a tetramer of spheres with R_0 = 19.3 Å and also gives the overall dimensions of the spheroid used to approximate the different structurally arranged n-mers. The computed values are for infinite dilution, and thus a comparison with experiment should be made with this in mind. The experimentally determined $s_{20,w}$ values for aggregates would be greater at infinite dilution if the aggregates could be maintained at high dilution because of the typical concentration dependence of sedimentation coefficients for noninteracting systems (Schachman, 1959). The computed values for dimer and trimer are in good agreement with the observed $s_{20,w}$ value at a pH of 7–9, and thus, in the narrow concentration range of 0.2–0.4 mg/mL, LeIF-A appears to be aggregating from a monomer up to a trimer. These estimates of the sedimentation coefficient should not be construed as evidence for a simple monomer to trimer aggregation. At concentrations greater than 1 mg/mL, the sedimentation coefficients are greater than 4.0, and thus the aggregation may proceed to larger aggregates than trimer. The intrinsic coefficient for a particular aggregate depends on the geometry of the structure formed (see Table II), and thus, it is difficult to assess the particular contribution of higher order aggregates. However, the concentration dependence of $s_{20,w}$ at pH 6.9–7.0, closed circles shown in Figure 7, does provide additional insight into the details of the aggregation behavior. In the concentration range of 0.05–6.0 mg/mL, the sedimentation coefficient increases with increasing concentration but appears to plateau at the higher concentration limit. The concentration dependence of $s_{20,w}$ for a noninteracting single-sedimenting species results in a curve with a negative slope; i.e., the sedimentation coefficient decreases with increasing concentration (Schach-

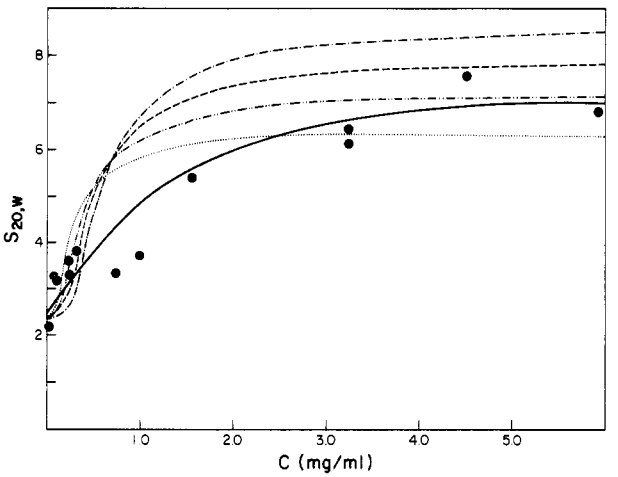

FIGURE 7: Corrected sedimentation coefficients (●) ($s_{20,w}$) for human LeIF-A at pH 6.9–7.0, 23 °C [I = 0.01 M K(H)PO_4 + 0.09 M KCl], as a function of the loading protein concentration. Curves are computer-simulated weight-average sedimentation coefficients. Monomer molecular weight = 19 400, $\bar{V}_p$ = 0.73, and ρ and η are for water at 20 °C. The intrinsic sedimentation coefficient of monomer = 2.4 S and $s_{n\text{-mer}} = s_{monomer} n^{2/3}$. For monomer to n-mer tight association, $K(n)$ for $nM \rightleftharpoons M_n$ was set equal to 1000.0, and all $K(I)$, I = 2, n − 1 were set equal to 0.00001: (---) n = 8; (- - -) n = 7; (-·-·-) n = 6; (···) n = 5. The solid line through the data points was computed for a monomer to octamer association. $K(8)$ = 2000.0, $K(7)$ = 500.0, $K(6)$ = 400.0, and $K(5) = K(4) = K(3) = K(2)$ = 4.0.

man, 1959; Gilbert, 1963). The behavior of the s vs. concentration data (Figure 7) is typical of a rapidly reversibly aggregating system (Gilbert, 1963) where the mass action of the polymerization dominates the hydrodynamic behavior of individual aggregates. As expected for a reversibly aggregating system, at low concentrations, there is a decrease in the sedimentation coefficient to a value of 2.0 S which is the value for LeIF-A monomer. At higher concentrations, the data appear to plateau, and this suggests that the aggregation is not an indefinite assembly.

Computations of the weight-average sedimentation coefficient as a function of loading concentration are included with the experimental data in Figure 7. It is not possible to compute a curve which gives a reasonable fit if the aggregation model is assumed to be a tight monomer to n-mer aggregation. Computations are shown for 8-, 7-, 6-, and 5-mer where for a particular monomer to n-mer aggregation $K(n) = 1000$ and $K(I) = 0.00001$ for $I = 2, n - 1$. In all cases, the curves rise too rapidly at low concentrations. The curves also predict the presence of a sigmoidal shape at very low concentrations, but unfortunately, the scatter in the experimental data precludes a good comparison in this range of the curve. A reasonable fit to the data shown by the solid line in Figure 7 was obtained by setting $K(2) = K(3) = K(4) = K(5) = 4.0$, $K(6) = 400.0$, $K(7) = 500.0$, and $K(8) = 2000.0$. This is obviously not a unique solution but does illustrate that the data can be fit with a truncation model up to octamer provided intermediates are included in the computation.

Conclusions regarding what is the largest aggregate in the assembly scheme cannot be made by comparing the maximum s values computed to those experimentally determined because of the variation with geometry of the intrinsic sedimentation coefficient of the aggregates (Table II). However, the computations assuming equal frictional ratios for all aggregates strongly suggest that intermediates are present in the aggregation scheme. Further elaboration by molecular weight determinations by using the sedimentation equilibrium technique will be required.

Role of Ionizing Groups in LeIF-A Polymerization. These results show that there exists a linkage between the ionization state of LeIF-A and self-polymerization. The time-dependent variation of pH during reverse titration from pH 7.0 to 6.1 (Figure 1) and the increase in sedimentation coefficient occur over the same range of pH values (Figure 5). The titration curve of LeIF-A from pH 7.0 to 9.5 can be computed from the amino acid composition of LeIF-A only if three amino acid residues (Tyr or Lys) are assigned depressed pK values of 7.0. Since the sedimentation coefficient above this pH is at least 4.0 S, these ionizing groups have depressed pK values in the aggregated state.[2] As the pH is decreased from 7.0 to 5.0, depolymerization occurs (Figure 5), and the pK values increase for these groups. This is reflected in the time-dependent increase in pH on reverse titration (arrows and encircled crosses, Figure 1) since an increase in pK values would result in the binding of protons.

The amino acid residues with depressed pK values in the polymerized state may be lysine or tyrosine residues. Arginine appears unlikely to have depressed pK values below 7.0 because of the large expense in free energy required to bury a deprotonated arginine residue. A substantial amount of free energy ($\sim$4 kcal/mol) would be required to bury an unprotonated lysine residue at alkaline pH values. However, this free energy might be gained from favorable interactions between protein monomers during assembly. Tyrosine residues may be involved by virtue of a stabilization of the phenolate anion, resulting in a depressed pK value. Spectrophotometric titrations of tyrosine ionization in LeIF-A are currently in progress and should elucidate the contribution from this residue. Subtraction of the tyrosine titrations from the potentiometric data will result in titration data for the ϵ-amino groups.

It is also possible that counterion binding to specific protein sites could result in apparent abnormally titrating residues. Since ion binding data are not currently available for LeIF-A, the titration curves were computed from the raw data by assuming that no binding takes place. Further experimentation will be required to determine the role of counterion binding on assembly as well as hydrogen ion binding.

[2] The actual value of these pK values in the aggregated state has not been determined. An arbitrary pK value of 7.0 was used in the computation of the titration curve from pH 7.0 to 9.5. Any pK value less than 7.0 would result in good agreement with the data.

Conclusions

In summary, this study demonstrates that human LeIF-A aggregates reversibly as a function of pH and concentration from monomer up to perhaps octamer with the presence of intermediate size aggregates. This self-polymerization also appears to be linked to the ionization of three basic residues with depressed pK values in the aggregated state.

A complete understanding of the aggregation behavior of this potentially useful pharmaceutic will be extremely important in regard to its stability and storage behavior at high concentrations. With regard to the mode of action, our knowledge of interferon–receptor binding is limited, and the role of self-polymerization at physiological pH due to local concentration effects at cell surfaces is obviously open to question, especially in regard to cell surface receptor mobility. Moreover, the possibility of an immune response may also be related to the propensity of the molecule to associate. A recent theory on immune response deals with the clustering of cell-surface receptors as a key event for eliciting antibody synthesis (Vogelstein et al., 1982), and the ability of antigen to self-associate may enhance such an effect. A complete understanding of the aggregation behavior of LeIF-A in terms of solution conditions and thermodynamic parameters will be necessary in order to use this drug in the safest and most effective way possible.

Acknowledgments

I thank Professor Howard Schachman (University of California, Berkeley) for his helpful comments and generous use of his model E ultracentrifuge and laboratory facilities. The use of the model E ultracentrifuge and laboratory facilities at the University of Connecticut, Storrs, through the generosity of Professors Todd Schuster and Emory Braswell (University of Connecticut) is also gratefully acknowledged. The assistance of John Steckert (University of Connecticut) in the initial UV-scanner centrifuge experiments is also gratefully appreciated. Purification of some of the interferon samples used was by Dr. Robert Hershberg and Dr. Ronald Wetzel (Genentech), and their contribution is appreciated. Critical reading of the manuscript by Dr. Howard Levine (Genentech) is also acknowledged.

References

Asai, H. (1961) *J. Biochem. (Tokyo) 50*, 182–189.

Bailey, K. (1948) *Biochem. J. 43*, 271–279.

Bewley, T. A., Levine, H. L., & Wetzel, R. (1982) *Int. J. Pept. Protein Res. 20*, 93–96.

Bloomfield, V., Dalton, W. O., & Van Holde, K. E. (1967) *Biopolymers 5*, 135–148.

Caspar, D. L. D. (1963) *Adv. Protein Chem. 18*, 37–121.
Cox, D. J. (1978) *Methods Enzymol. 48*, 212–242.
DeBruin, S. H., & Van Os, G. A. T. (1968) *Recl. Trav. Chim. Pays-Bas 87*, 861–872.
Fritsch, C., Witz, J., Abou Haidar, M., & Hirth, L. (1973) *FEBS Lett. 29*, 211–214.
Gilbert, G. A. (1959) *Proc. R. Soc. London, Ser. A 250*, 377–388.
Gilbert, G. A. (1963) in *Ultracentrifugal Analysis in Theory and Experiment* (Williams, J. W., Ed.) pp 73–79, Academic Press, New York.
Goeddel, D. V., Yelverton, E., Ullrich, A., Heyneker, H. L., Miozzari, G., Holmes, W., Seeburg, P. H., Dull, T., May, L., Stebbing, N., Crea, R., Maeda, S., McCandliss, R., Sloma, A., Tabor, J. M., Gross, M., Familletti, P. C., & Petska, S. (1980) *Nature (London) 287*, 411–416.
Goeddel, D. V., Leung, D. W., Dull, T. J., Gross, M., Lawn, R. M., McCandliss, R., Seeburg, P. H., Ullrich, A., Yelverton, E., & Gray, P. W. (1981) *Nature (London) 290*, 20–26.
Hill, T. L. (1955) *Arch. Biochem. Biophys. 57*, 229–239.
Kauzmann, W. (1959) *Adv. Protein Chem. 14*, 1–63.
Kirkwood, J. G. (1949) *Recl. Trav. Chim. Pays-Bas 68*, 649–660.
Kirkwood, J. G. (1954) *J. Polym. Sci. 12*, 1–14.
Linderstrøm-Lang, K. (1924) *C. R. Trav. Lab. Carlsberg 14* (*7*), 1–30.
Mantei, N., Schwarzstein, M., Streuli, M., Panem, S., Shigekaszu, N., & Weissmann, C. (1980) *Gene 10*, 1–10.
Marini, M. A., & Martin, C. J. (1980) *Anal. Lett. 13* (*B2*), 93–103.
Matthew, J. B., Friend, S. H., Botelho, L. H., Lehman, L. D., Hanania, G. I. H., & Gurd, F. R. N. (1978) *Biochem. Biophys. Res. Commun. 81*, 416–421.
Oosawa, F., & Asakura, S. (1975) *Thermodynamics of the Polymerization of Protein*, Academic Press, New York.
Perrin, F. (1936) *J. Phys. Radium 7*, 1–14.
Schachman, H. K. (1959) *Ultracentrifugation in Biochemistry*, Academic Press, New York.
Shire, S. J., Hanania, G. I. H., & Gurd, F. R. N. (1974a) *Biochemistry 13*, 2967–2974.
Shire, S. J., Hanania, G. I. H., & Gurd, F. R. N. (1974b) *Biochemistry 13*, 2974–2979.
Staehelin, T., Durrer, B., Schmidt, J., Takacs, B., Stocker, J., Miggiano, V., Stähli, C., Rubinstein, M., Levy, W. P., Hershberg, R., & Petska, S. (1981) *Proc. Natl. Acad. Sci. U.S.A. 78*, 1848–1852.
Stewart, W. E., II (1979) *The Interferon System*, Springer-Verlag, New York.
Streuli, M., Nagata, S., & Weissman, C. (1980) *Science (Washington, D.C.) 209*, 1343–1347.
Tanford, C. (1961) *Physical Chemistry of Macromolecules*, pp 457–525, Academic Press, New York.
Tanford, C. (1962) *Adv. Protein Chem. 17*, 69–165.
Tanford, C., & Roxby, R. (1972) *Biochemistry 11*, 2192–2198.
Van Os, G. A. J., DeBruin, S. H., & Janssen, L. H. M. (1972) *J. Electroanal. Chem. Interfacial Electrochem. 37*, 303–311.
Vogelstein, R., Dintzis, R. Z., & Dintzis, H. M. (1982) *Proc. Natl. Acad. Sci. U.S.A. 79*, 395–399.
Wetzel, R. (1981) *Nature (London) 289*, 606–607.
Wetzel, R., Perry, L. J., Estell, D. A., Lin, N., Levine, H. L., Slinker, B., Fields, F., Ross, M. J., & Shively, J. (1981) *J. Interferon Res. 1*, 381–390.

Evidence for Tertiary Structure in Aqueous Solutions of Human β-Endorphin As Shown by Difference Absorption Spectroscopy†

Thomas A. Bewley* and Choh Hao Li

ABSTRACT: The presence of a distinct tertiary structure in aqueous solutions of human β-endorphin has been demonstrated by difference absorption spectroscopy of thermolysin digests of the hormone and synthetic analogues. The results demonstrate that the α-amino group of Tyr[1], Lys[28], and some residue(s) between Thr[6] and Ser[10] are involved in forming and stabilizing the folded form of the molecule. Although a peptide corresponding to the first nine residues of human β-endorphin shows definite evidence of tertiary structure, the pentapeptide methionine-enkephalin does not.

The enkephalins (EK)[1] and endorphins (EP) are important, naturally occurring opioid peptides of animal origin. EK's are pentapeptides containing an NH_2-terminal tyrosine (Hughes et al., 1975). The EP's are larger and contain an EK sequence for the first five residues from the NH_2 terminus (Li, 1981). CD studies have suggested that conformation may play some role in the biological activities of EP (Li, 1981).

Although a considerable amount of α-helical structure has been reported for EP in various nonpolar solvents (Li, 1981; Yang et al., 1977; Hollősi et al., 1977; Jibson & Li, 1981; Wu et al., 1979), NMR and CD studies did not find significant

† From the Hormone Research Laboratory, University of California, San Francisco, California 94143. *Received October 22, 1982.* This work was supported in part by grants from the National Institutes of Health (AM-18677 and GM-2907) and the National Institutes of Mental Health (MH-30245).

[1] Abbreviations: EK, enkephalin; EP, endorphin; β_h-EP, human β-endorphin; β_c-EP, camel β-endorphin; CD, circular dichroism; NMR, nuclear magnetic resonance; UV, ultraviolet; ϵ_M, molar extinction coefficient; $\Delta\epsilon_M$, change in molar extinction coefficient of a difference spectral maximum; $A_{cm}^{0.1\%}$, absorptivity of a 1.0 mg/mL solution through an optical path of 1.0 cm; E/S, enzyme to substrate ratio; HPLC, high-performance liquid chromatography; SEM, standard error of the mean. The usual three letter codes for the amino acids are used, with superscripts indicating positions within the EP sequence.

0006-2960/83/0422-2671$01.50/0